New Electron Delocalization Tools to Describe the Aromaticity in Porphyrinoids

Irene Casademont-Reig, Tatiana A Woller, Julia Contreras-García, Mercedes A Alonso, Miquel Torrent-Sucarrat, Eduard Matito

Journal Name

ARTICLE

New Electron Delocalization Tools to Describe the Aromaticity in Porphyrinoids

Received 00th January 20xx,
Accepted 00th January 20xx

DOI: 10.1039/x0xx00000x

www.rsc.org/

Irene Casademont-Reig,[a,†] Tatiana Woller,[b,†] Julia Contreras-García,[c] Mercedes Alonso,[b, ‡] Miquel Torrent-Sucarrat,[a,d,‡] Eduard Matito,[a,d, ‡]

The role of aromaticity in porphyrinoids is a current subject of debate due to the intricate structure of these macrocycles, which in some cases adopt Hückel, Möbius and even figure-eight conformers. One of the main challenges in these large π-conjugated structures is identifying the most conjugated pathway because, among aromaticity descriptors, there are very few that can be applied coherently to this variety of conformers. In this paper, we have investigated the conjugated pathways in nine porphyrinoid compounds using several aromaticity descriptors, including BLA, BOA, FLU and HOMA, as well as the recently introduced AV1245 and AV_{min} indices. All the indices agree on the general features of these compounds, such as the fulfillment of Hückel's rule or which compounds should be more or less aromatic from the series. However, our results evince the difficulty in finding the most aromatic pathway in the macrocycle for large porphyrinoids. In fact, only AV_{min} is capable of recognizing the annulene pathway as the most aromatic one in the nine studied structures. Finally, we study the effect of the exchange in DFT functionals on the description of the aromaticity of the porphyrinoids. The amount of exact exchange quantitatively changes the picture for most aromaticity descriptors, AV_{min} being the only exception that shows the same qualitative results in all cases.

1 Introduction

Aromaticity is a ubiquitous concept in chemistry that covers a large number of properties including energy stabilization, bond-length equalization, exalted magnetic properties and electron conjugation and delocalization.[1-6] As many other chemical concepts (chemical bonding, electronegativity, bond order, hardness, electron population, etc.), the aromaticity is not a quantum observable and it lacks a physical basis. This fact results in a plethora of aromaticity indices (energetic, structural, magnetic and electronic) reported in the literature,[2-4, 6, 7] which have been successfully applied to explain countless chemical phenomena. For this reason, it is recommended to study the multidimensional phenomenon of aromaticity with a set of descriptors based on different criteria.[6, 8-12]

However, the multidimensional character of aromaticity should not prevent from a critical analysis of aromaticity descriptors.[10, 13-15] Recently, Feixas *et. al*[10, 15] have designed a series of tests to evaluate the performance of aromaticity indices in organic and inorganic molecules, but the study of macrocycles was not among the tests suggested. In this regard, porphyrinoids can be considered one of the most stringent test beds for the aromaticity descriptors along three main different lines: a) identifying the most aromatic pathway; b) describing aromaticity in non-planar compounds; c) computational method dependency. In the following paragraphs, these three factors are addressed in detail.

The porphyrinoids contain several heterocycles and many multiple π-conjugation pathways can be defined. Then, one of the main issues to describe the aromaticity in porphyrinoids is to select the macrocyclic conjugation pathway (or pathways) to study. To this aim, porphyrinoids were traditionally interpreted as annulenes, *e.g.* porphine was considered as a tetraaza[18]annulene system.[16, 17] This approximation is called the annulene model; *i.e.* the pathway is selected avoiding the NH in pyrrole and the outer CH=CH groups of imine rings (see some examples of annulene pathways in Figure 1, illustrated in bold). Conversely, several authors[18-27] have concluded that all the π electrons of the macrocycles are necessary for a correct description of aromaticity in porphyrinoids and that the individual pyrrolic subunits (and not the imine rings) determine the global aromatic character of the macrocycle. For instance, in the case of porphine, it has been reported that it is necessary to consider all the 22 π electrons and not only the 18 π electrons of the annulene pathway for a correct description of its aromaticity.[28] From these discrepancies, it is possible to conclude that it is essential to search

[a] *Kimika Fakultatea, Euskal Herriko Unibertsitatea (UPV/EHU), and Donostia International Physics Center (DIPC), P.K. 1072, 20080 Donostia, Euskadi, Spain*
[b] *Eenheid Algemene Chemie (ALGC). Vrije Universiteit Brussel (VUB), Pleinlaan 2, 1050 Brussels (Belgium)*
[c] *Sorbonne Universités, UPMC Univ. Paris, UMR 7616 Laboratoire de Chimie Théorique, CNRS, UMR 7616, LCT 75005, Paris (France).*
[d] *Ikerbasque, Basque Foundation for Science, María Díaz de Haro 3, 6º, 48013 Bilbao, Euskadi, Spain.*

† These authors contributed equally to this work.

‡ Email: Mercedes.alonso.giner@vub.be, miqueltorrentsucarrat@gmail.com and ematito@gmail.com

Electronic Supplementary Information (ESI) available: This material is available free of charge via the Internet at http://www.rsc.org. The Electronic Supplementary Information is available free of charge on the RSC Publications website. See DOI: 10.1039/x0xx00000x

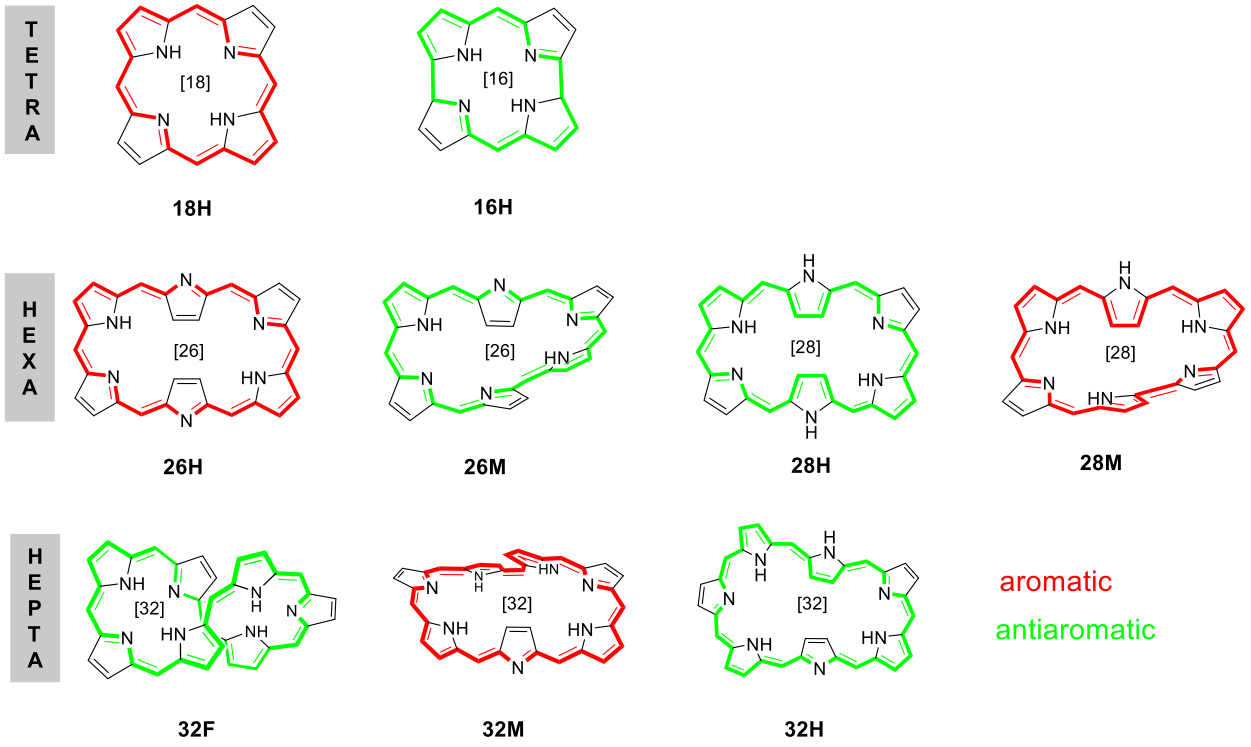

Figure 1. Hückel (H), Möbius (M) and figure-eight (F) conformations of selected porphyrinoids and their expected aromaticity according to the annulene model. The annulene-type conjugation pathway is depicted with bold colored bonds (red stands for aromatic and green for antiaromatic).

for new aromaticity descriptors that are able to select in an accurate way (ideally also unambiguous) the most aromatic pathway from a π-electron macrocyclic structure.

It is important to keep in mind that most of the aromaticity indices, such as the harmonic oscillator model of aromaticity (HOMA) and the nuclear-independent chemical shifts (NICS), have been conceived to describe the aromaticity of planar structures. Thus, an additional problem appears when the porphyrinoid structure shows a nonplanar geometry.[29, 30] Within this context, it is necessary to put a special emphasis on expanded porphyrins. These systems present a conformational flexibility that allows them to achieve different π-conjugation topologies (namely, Möbius, Hückel and twisted-Hückel) with distinct aromaticities, as well as different electric, magnetic and conductance properties.[31-35] For instance, the switch between different topologies (*e.g.* the Hückel planar, single twisted Möbius, figure eight, and triply twisted Möbius) can be achieved by changing external conditions, such as the temperature, the solvent, the redox potential or through metalation and photoexcitation.[36-41]

According to the Hückel rule, a planar (or with an even number of half-twists) singlet π-conjugated system with 4*N*+2 π-electrons is aromatic, whereas with 4*N* π-electrons is antiaromatic. On the other hand, Heilbronner[42] predicts that the Hückel rule is reversed for a planar π-conjugated system with an odd number of half-twists; *i.e.* a singlet Möbius system with 4*N*+2 (4*N*) π electrons is antiaromatic (aromatic). This diversity of aromatic patterns with different topologies can be increased by a factor of two if one considers triplet states because, according to Baird's rule,[43, 44] the aromaticity/antiaromaticity electron counting rule of the singlet ground state is reversed for the lowest ππ* triplet state. Expanded porphyrins (and to a minor degree annulenes) present all these features.[45-54] In this sense, it is not unexpected that expanded porphyrins are among the most challenging test beds for aromaticity descriptors. It should be pointed out that several works[20, 55-62] have recently analyzed the aromaticity of expanded porphyrins with different topologies and number of π electrons using various aromaticity indices based on the energetic, magnetic, structural, and reactivity criteria.

The last problem to describe the aromaticity of porphyrinoids is the critical role of the selected density functional approximations (DFA) to evaluate geometric, energetic and magnetic properties.[63-66] For instance, for expanded porphyrins, it has been reported that some DFA overemphasize the delocalization of conjugated systems, which results in more stable and bond-equalized structures.[66] In this regard, it is worth noting that this phenomenon has also been observed in annulenes.[67-70] The effect of the method in aromaticity descriptors remains unexplored and will be addressed in this work.

Many of the current aromaticity indices cannot be easily applied in macrocycles, motivating the definition of new aromaticity descriptors.[71, 72] One of us[71] has recently proposed the AV1245 index, which consists in the average of the 4-center multicenter indices (MCI) values along the ring that keep a positional relationship of 1, 2, 4, 5. It measures the extent of transferability of the delocalized electrons between bonds 1-2 and 4-5, which is expected to be large in aromatic molecules. The main advantages of AV1245 are that it does not rely on reference values, does not

suffer from large numerical precision errors and it does not present any limitation on the nature of atoms, the molecular geometry or the level of calculation.

Herein, we report a theoretical investigation on the aromaticity of nine porphyrinoid compounds (see Figure 1) using three DFA (B3LYP, M06-2X and CAM-B3LYP) and six aromaticity descriptors (AV1245, AV_{min}, BLA, BOA, FLU and HOMA). In order to test the new electron delocalization tools (AV1245 and AV_{min}), and to provide deeper insight into the evaluation of porphyrinoids' aromaticity and their three major challenges (*vide supra*), three different studies have been performed. Firstly, all the possible pathways in porphine have been evaluated using the six aromaticity descriptors and the most aromatic pathway has been identified. Secondly, the values of the aromatic indices for the annulene pathway of all the studied molecules are analyzed. Finally, the influence of the exchange-correlation functional in the values of the different aromaticity indices has been discussed.

2 Methodology

In this section, we will review several aromaticity measures that can be applied to find the most conjugated pathway in porphyrins. Many other popular measures of aromaticity such as the NICS,[73] the aromatic stabilization energies,[7] the magnetic susceptibility exaltation[74] or the relative hardness[65] provide *global* measures of aromaticity and cannot be employed to find the most aromatic pathway in a macrocycle.

Hereafter, we will indicate the coordinates of the electron using the short-hand notation $\mathbf{1} \equiv (\vec{r}_1, \sigma_1)$ and $d_1 \equiv d\vec{r}_1 d\sigma_1$ for the electron positions and their derivatives and we will assume a single-determinant wavefunction (for a more general approach we suggest Ref. 75). Let us consider a ring structure consisting of *n* atoms, represented by the string $\mathcal{A} = \{\mathcal{A}_1, \mathcal{A}_2, \ldots, \mathcal{A}_n\}$, whose elements are ordered according to the connectivity of the atoms in the ring. In order to illustrate the performance of electron delocalization indices, we select three archetype molecules: benzene, cyclohexane and three geometries of cyclohexatriene with variable bond-length alternation.

First of all, we will review the concepts of an *atom in a molecule* (AIM), electron delocalization and bond orders, which are employed in the definition of the electronic indices of aromaticity. In order to estimate the aromaticity of molecules, we need to define an AIM, so as to measure the electron delocalization among the atoms in the ring. In this work, we will define the AIM using the quantum theory of atoms in molecules (QTAIM)[76] that defines the boundaries of an atom using the topology of the electron density. The QTAIM is among the most reliable definitions of an AIM, providing good estimates of bond orders in difficult cases[77-83] and trustworthy results for aromaticity indices.[84] As a measure of electron delocalization, we will employ Bader's definition[85] that estimates the electron delocalization as the variance of the atomic population, $\delta(A)$. From this definition, one can provide a measure of the bond order based on the covariance of the populations of atoms *A* and *B*,[78, 86] commonly known as the delocalization index (DI),

$$\delta(A,B) = 2\int_A \int_B d\mathbf{1}d\mathbf{2}\rho_{xc}(\mathbf{1},\mathbf{2}) = -2cov(N_A, N_B) \quad , \qquad (1)$$

where $\rho_{xc}(\mathbf{1},\mathbf{2})$ is the exchange-correlation density and N_A is the atomic population of atom *A*. $\delta(A)$ is the variance of the atomic population and it is given by $\delta(A) = N_A - \delta(A,A)/2$. For single-determinant wave functions (Hartree-Fock or Kohn-Sham DFT), the calculation of N_A and $\delta(A,B)$ only requires the atomic-overlap matrices (AOMs),

$$S_{ij}(A) = \int_{A_1} d\mathbf{1}\phi_i^*(\mathbf{1})\phi_j(\mathbf{1}) \quad , \qquad (2)$$

where $\phi_i(\mathbf{1})$ is the orbital *i* of the set of orbitals in terms of which we expand the density and the exchange-correlation density. Some authors have found a link between the DI and the interaction energy of two atoms.[87-89] In Table 1, the DI values for several molecules are collected. Cyclohexane shows the typical value of δ(C, C) of a non-aromatic molecule which equals 1, as the bond involves only sigma orbitals. The structures of cyclohexatriene show some δ(C, C) close to one, and others close to two, indicating an alternation of single and double bonds, typical of antiaromatic molecules, whereas benzene gives δ(C, C) = 1.4, which is halfway between single and double bonds and it is the typical signature of the conjugated bonds present in aromatic molecules.

Table 1. DI values and aromaticity indices for benzene, cyclohexane and three structures of cyclohexatriene calculated at the B3LYP/6-311G(d,p) level of theory.

		$\delta(C_1,C_2)$	$\delta(C_2,C_3)$	FLU	BOA	HOMA	BLA	MCI	AV1245	AV_{min}
Benzene 		1.39	1.39	0.000	0.000	0.991	0.000	0.073	10.72	10.72
Cyclohexane 		0.98	0.98	0.092	0.000	-4.637	0.000	0.000	-0.01	0.01
Cyclohexatriene 	a/b=0.9	1.12	1.59	0.029	0.472	-18.024	0.204	0.050	8.16	8.16
	a/b=0.8	0.97	1.76	0.082	0.797	-31.266	0.408	0.017	3.70	3.70
	a/b=0.7	0.86	1.89	0.138	1.037	-50.540	0.622	0.009	2.18	2.18

One of the most popular indicators of aromaticity is the bond-length alternation (BLA), which compares the average of bond lengths of consecutive bonds in a ring,

$$BLA\ (\mathcal{A}) = \frac{1}{n_1}\sum_{i=1}^{n_1} r_{A_{2i-1},A_{2i}} - \frac{1}{n_2}\sum_{i=1}^{n_2} r_{A_{2i},A_{2i+1}} \quad , \qquad (3)$$

where $n_1 = \lfloor (n+1)/2 \rfloor$, $n_2 = \lfloor n/2 \rfloor$; the symbol $\lfloor x \rfloor$ standing for the floor function of *x*, that returns the largest integer less than or equal to *x*. The BLA directly measures the bond-length equalization expected in aromatic circuits and it does not rely on reference values. In Table 1, we see that benzene and cyclohexane do not exhibit bond-length alternation, whereas cyclohexatriene increases the value of BLA with bond-length alternation. However, the BLA is built upon the premise that the bond-length alternation (*i.e.* a geometrical feature) reflects the distribution of electron pairs on the conjugated circuit. For this reason, some people prefer an electronic-structure equivalent of the BLA, the bond-order alternation (BOA), which uses the bond order (or electron-sharing index[78]) instead of the bond length,

$$BOA\ (\mathcal{A}) = \frac{1}{n_1}\sum_{i=1}^{n_1} \delta(A_{2i-1},A_{2i}) - \frac{1}{n_2}\sum_{i=1}^{n_2} \delta(A_{2i},A_{2i+1}) \quad , \quad (4)$$

where $\delta(A,B)$ is a given measure of the bond order between atoms *A* and *B*. Unlike the atomic charges,[90] the bond orders are much less dependent on the method and the basis set used[91] and, therefore, aromaticity indices based on bond orders[92] are not highly dependent on the level of theory employed. The values of the BOA are collected in Table 1 and show the same trend as the BLA values for these systems.

An alternative geometry-based index is the widely used harmonic oscillator model of aromaticity (HOMA) proposed by Kruszewski and Krygowski.[93] The HOMA uses some reference bond lengths, R_{opt}, for which the compression energy of the double bond and expansion energy of the single bond are minimal according to the harmonic potential model. The expression of HOMA is based on the differences between the reference and the actual bond lengths within the ring structure:

$$HOMA\ (\mathcal{A}) = 1 - \frac{1}{n}\sum_{i}^{n} \alpha_i (R_{opt} - R_{A_i,A_{i+1}})^2 \quad , \qquad (5)$$

where α_i is an empirical constant fixed to give values close to one for aromatic species, and small or large negative values for non-aromatic and antiaromatic molecules (see Table 1). For C-C bonds, α_i = 257.7 and R_{opt} = 1.388Å, whereas α_i = 93.52 and R_{opt} = 1.334Å for C-N bonds.[94]

Just as BOA is the quantum-chemical equivalent of BLA, the aromatic fluctuation index (FLU) is constructed to go beyond the bond-length information in the analysis of aromaticity of a ring.[95, 96] The FLU expression only employs information about the electron delocalization of the atoms in the ring,

$$FLU(\mathcal{A}) = \frac{1}{n}\sum_{i=1}^{n} \left[\left(\frac{\delta(A_i)}{\delta(A_{i-1})} \right)^{\alpha} \left(\frac{\delta(A_i,A_{i-1}) - \delta_{ref}(A_i,A_{i-1})}{\delta_{ref}(A_i,A_{i-1})} \right) \right]^2 , \quad (6)$$

where $\delta_{ref}(A_i,A_j)$ are taken from some reference aromatic molecules where the bonding pattern A_i-A_j occurs in the aromatic ring (for instance, the C-C delocalization is taken from benzene and the C-N delocalization is taken from pyridine), and

$$\alpha = \begin{cases} 1 & \delta(A_{i-1}) \le \delta(A_i) \\ -1 & \delta(A_i) < \delta(A_{i-1}) \end{cases} \quad . \qquad (7)$$

The FLU index is close to zero for aromatic molecules and takes large values for non-aromatic and antiaromatic molecules (see Table 1). It is worth to mention that the FLU has been already used to account for the aromaticity in porphyrins.[97] Unfortunately, the aromaticity indices based on references do not actually measure aromaticity but the similarity with respect to some aromatic molecule (or patterns found in aromatic molecules). In this sense, HOMA and FLU are not adequate to describe reactivity because they will always predict a loss of aromaticity when the bond distance or the delocalization, respectively, change with respect to the reference value.[14] For instance, in the case of the Diels-Alder reaction they cannot recognize the transition state (TS) as the most aromatic point along the reaction path because the product, cyclohexene, is more similar to benzene (the reference molecule for C-C bonds) than the TS, which shows large C-C distances and small DIs in the bonds that will be formed.[13] In addition, several studies pointed out that the HOMA index needs to be applied with caution in expanded porphyrins because the HOMA differences between aromatic and antiaromatic conformations are very small and the HOMA index behaves qualitatively different for aromatic and antiaromatic species.[62, 98]

The most reliable indices of aromaticity are actually based on multicenter electron delocalization measures.[10, 15] The first such measure is due to Giambiagi and measures the electron delocalization along the ring,[99]

$$I_{ring}(\mathcal{A}) = \sum_{i_1,i_2\ldots i_n}^{occ} S_{i_1 i_2}(A_1) S_{i_2 i_3}(A_2) \ldots S_{i_n i_1}(A_n) \quad . \qquad (8)$$

This measure was extended to include all the delocalization patterns across the ring (*i.e.* it uses not only the Kekulé structure but all the possible arrangements of the atoms in the string $\mathcal{A}$),[100]

$$MCI(\mathcal{A}) = \sum_{\mathcal{P}(\mathcal{A})} I_{ring}(\mathcal{A}) = \sum_{\mathcal{P}(\mathcal{A})} \sum_{i_1,i_2\ldots i_n}^{occ} S_{i_1 i_2}(A_1) S_{i_2 i_3}(A_2) \ldots S_{i_n i_1}(A_n) \ , \qquad (9)$$

where $\mathcal{P}(\mathcal{A})$ stands for the *n*! permutations of the elements in the string $\mathcal{A}$. Both I_{ring} and MCI produce large values for aromatic molecules, small values for non-aromatic molecules and negative values for some antiaromatic molecules (see Table 1).[101] These indices are ring-size dependent but proper normalization has been recently suggested.[102] Unfortunately, the cost and the numerical error associated with these quantities grow with the ring size and their calculation for rings of more than twelve atoms poses a serious computational challenge.[71]

Recently, we have put some effort in overcoming these drawbacks, resulting in the definition of a new electronic

aromaticity index for large circuits, the AV1245 index.[71] Based upon the study of long-range delocalization patterns in aromatic molecules,[103, 104] the AV1245 index measures the average delocalization in bonds 1-2 and 4-5 along a ring of more than six members. To this aim, we average out the four-center MCI values (including atoms in positions 1, 2, 4 and 5) of each consecutive five-atom fragment in the circuit. In the framework of intermolecular conjugation, we have found that the AV_{min} (the minimal absolute value of the aforementioned four-center MCI values along the ring) can be used to characterize the high dispersive bands in conjugated polymers.[105] Both AV_{min} and AV1245 show large numbers for aromatic molecules (AV1245 ≈ 11 for benzene) and small numbers for antiaromatic and non-aromatic molecules. In this sense, the combined information of BOA and AV1245/AV_{min} helps distinguishing the latter situations.

Finally, we should also mention that the electron density of delocalized bonds has been recently used as an additional electronic criterion to account for aromaticity in large circuits.[72]

3 Computational methods

The geometries of the selected porphyrinoids (see the structures in Fig. 1) have been fully optimized and characterized by harmonic vibrational frequency calculations with B3LYP,[106, 107] M06-2X[108] and CAM-B3LYP[109] functionals in combination with the 6-311G(d,p) basis set.[110, 111] The initial structures of the Hückel, Möbius and figure-eight topologies of [26]- and [28]-hexaphyrins and [32]-heptaphyrin[112] have been obtained from our previous works (notice that the meso substituents in Fig. 1 are hydrogen atoms).[58, 63, 64, 66] The geometry optimizations and frequencies of the DFT methods were performed with the Gaussian 09 software package.[113] The calculation of the electronic aromaticity indices (AV1245, AV_{min}, BOA and FLU) uses a QTAIM atomic partition performed by the AIMAll software.[114] The AOM resulting from this partition (see Eq. 2) and the molecular geometries are input in the in-house ESI-3D code,[78, 92, 115] which provides AV1245, AV_{min}, BLA, BOA, DIs, FLU, HOMA and MCI values. The ESI-3D code is available upon request.

4 Results and discussion

We have performed calculations on nine porphyrinoid systems, collected in Fig. 1. First of all, we will analyze the simplest system, the porphine molecule (**18H** in Fig. 1), to illustrate the performance of the different measures of aromaticity studied in this work. We will choose CAM-B3LYP optimized structures to analyze the aromaticity of all porphyrinoid structures considered, however, in the last part of this section, we will also comment on the influence of the exchange-correlation functional in the values of the aromaticity descriptors. All the results obtained with B3LYP and M06-2X can be found in the Electronic Supplementary Information (see Tables S1 and S2).

In Table 2, the results for all the possible pathways in **18H** are collected. **18H** is composed of imine and pyrrole rings. The pathways differ on the route they follow upon passing through five-membered rings (5-MRs): they can pass through the C-N-C bonds (inner path, hereafter) or through the C-C bonds (outer path). We label the pathways using as many letters as 5-MRs the porphyrinoid structure has. These letters are 'i' for inner paths and 'o' for outer paths. We take the top left 5-MR of the structures in Fig. 1 and follow the clockwise direction to define the order of the 5-MRs in the molecule. According to this convention, the classical or annulene path in the **18H** system is labeled as 'oioi' (see the red pathway in Fig. 1). See Fig. S1 for drawings of all possible pathways in **18H**. The first entry in Table 2 displays the results for the annulene pathway in **18H**, showing that all aromaticity indices recognize this circuit as highly aromatic. However, by comparison with other pathways, we observe that only some indices (AV1245, AV_{min}, BLA and BOA) recognize the annulene pathway as the most aromatic one. In addition, we notice that BLA and BOA recognize the opposite path to the annulene model (*i.e.* 'ioio') as aromatic as the annulene pathway itself, which is somehow contradictory. On the other hand, AV1245 and AV_{min} identify the 'ioio' as the least aromatic pathway in **18H**. We have also computed the delocalization indices (DIs) for all the bonds in **18H** (see Fig. S2) and the DIs with largest values follow the annulene pathway.

In order to decide for the second most conjugated pathway, we should take the one predicted by the annulene model and choose a different route in one of the 5-MRs. The most reasonable choice consists in changing the route in the most aromatic 5-MR in the macrocycle, where the change of route is expected to be less important. Taking into account that our current MCI calculations predict that the imine rings within **18H** (MCI=0.024) are somewhat more aromatic than the pyrrole rings (MCI=0.022), we assume that the second most aromatic pathway corresponds to 'oooi' (see Table S3 of the Electronic Supplementary Information). Both AV_{min} and AV1245 predict this one as the second most aromatic pathway. If we follow this rule of choosing an alternative route on the next most aromatic 5-MR, we order the pathways as they are presented in Table 2. AV1245 and AV_{min} follow this very same order, suggesting that the local aromaticity of the 5-MRs calculated from MCI values is consistent with the description provided by these indices, which are based on four-center MCI calculations along the macrocyclic ring.

Table 2. Aromaticity indices for the different pathways in **18H**, calculated at the CAM-B3LYP/6-311G(d,p) level of theory.

Pathway[a)]	FLU	BOA	HOMA	BLA	AV1245	AV_{min}
oioi	0.010	0.000	0.872	0.000	2.16	1.28
oooi (2)	0.016	0.309	0.734	0.288	1.91	0.49
oooo	0.022	0.041	0.610	0.011	1.70	0.49
iioi (2)	0.008	0.367	0.917	0.313	1.57	0.13
ooii (4)	0.015	0.023	0.769	0.006	1.36	0.13
ooio (2)	0.021	0.372	0.637	0.270	1.17	0.13
iiii	0.006	0.000	0.968	0.000	0.91	0.13
iiio (2)	0.013	0.388	0.808	0.307	0.73	0.13
ioio	0.019	0.000	0.666	0.000	0.57	0.13

[a)] The number in brackets indicates the number of equivalent pathways.

We observe that AV_{min} provides the same value for some pathways because they share a given five-center fragment for which the four-center MCI absolute value turns out to be minimal. In such cases, since the AV_{min} value is identical, we assume the pathways are rather similar and if a distinction between them needs to be done, we suggest using AV1245 as a way to differentiate them.

However, the order of pathways we have just described for **18H** is not completely followed by either the topological or magnetic indices of aromaticity.[19-23, 25, 116] While these indices agree on the annulene pathway being, by far, the most conjugated one, their values for the second and third most aromatic pathways correspond to 'iioi' and 'oioo', respectively.[19] The latter puts forward that these indices prefer to choose alternative routes for pyrrole rings rather than for imine ones, as it was the case of AV1245 and AV_{min}. Interestingly, this fact is also in agreement with the 5-MRs aromaticity predicted by the topological and magnetic indices, which predict the pyrrole ring within **18H** as more aromatic than the imine ring. This rather simple example puts forward the difficulty of ordering the pathways in a porphyrinoid system according to their aromaticity. While most indices agree on the most aromatic pathway, the next most aromatic ones are quite difficult to classify and it seems that the aromaticity of the 5-MRs determines the aromaticity of the pathways. After all, aromaticity is a multidimensional phenomenon of which we are only measuring indirect consequences. We are not necessarily measuring the very same thing when we are comparing geometrical, electronic and magnetic indices of aromaticity and, therefore, some discrepancies are expected. [Cite 2D aromaticity]

In the following, we will be only concerned with the annulene pathway of the structures. Table 3 collects the values of the aromaticity indices for the annulene pathway of all selected porphyrinoids (Fig. 1). The indices that do not recognize the annulene pathway as the most aromatic one also include in parenthesis the values of the most aromatic pathway for comparison. First of all, we check whether the values of the indices reflect the global aromatic character expected in these systems. According to all the indices hereby studied, **18H** is the system with the most aromatic pathway and for **16H** the annulene pathway is predicted as having low aromaticity (as expected from a nonplanar antiaromatic system). In addition, all indices also agree on finding the annulene pathway in Hückel aromatic systems more aromatic than the annulene pathway in the corresponding Möbius antiaromatic systems (compare **26H** and **26M**) and *vice versa*: attributing a more aromatic character to the annulene pathway in Möbius aromatic systems than in the corresponding Hückel antiaromatic system (compare **28M** and **28H**, and **32M** and **32H**). Interestingly, the figure-eight structure of **32F** is predicted as an intermediate situation between **32H** and **32M**. Hence, in general, all the indices provide a reasonable description among the different conformers. However, when comparing the most aromatic pathway in the macrocycle many differences arise (*vide infra*).

The annulene model works fairly well in identifying the most aromatic pathway in simple free-base porphyrinoid systems, which are not protonated or deprotonated.[21] In addition, for these systems, the global aromatic character coincides with the aromaticity of the most conjugated pathway and, from a qualitative point of view, it can be determined by the number of π-electrons in this circuit.[21] In this sense, the systems selected in this work are expected to have the annulene pathway as the most aromatic one in the porphyrinoid structure. We have examined the DIs along the different pathways and we have found that in all cases except **16H**, the annulene path is the one with the largest DIs (see Electronic Supplementary Information). However, when we examine the aromaticity indices (see Table 3), we observe that only AV_{min} predicts the annulene pathway as the most aromatic one in all the studied porphyrinoids. In some cases, the most aromatic pathway presents values close to the annulene pathway and, therefore, one could argue that the indices perform qualitatively well. However, as the size of the porphyrinoid increases, the differences between the most conjugated pathway and the annulene one become larger. For instance, **32H**, **32M** and **32F** present pathways with very small BLA and BOA, which seem to suggest that these circuits are more aromatic than the annulene pathway. However, as we examine in greater detail the bond lengths and the DI patterns we realize that the small BLA and BOA values are due to the compensation of deviations from the average values between odd and even bonds (see Eqs. 3 and 4, respectively). In this sense, small values of BOA and BLA should be taken with caution, as they do not always indicate a lack of bond-length or bond-order alternation. Another important problem occurs in other indices based on averages, such as AV1245, FLU or HOMA. Some large specific deviations in bond orders, bond lengths and multicenter indices, which could hinder the conjugation along the pathway (and therefore, aromaticity), can be concealed as they are averaged with the rest of values. If the number of atoms in the pathway is relatively small, as it occurs in small organic rings, large individual deviations are easily spotted and, quite often, they importantly affect the average value. However, in large samples, *i.e.* in large expanded porphyrins, a few specific deviations are easily hidden. For these reasons, we believe AV_{min} is a better descriptor of the aromaticity than the other quantities considered in Table 3.

Finally, we focus on the effect of the density functional in the calculation of these electronic and structural aromaticity indices. There have been recent discussions in the literature concerning the role of the amount of the exact exchange in the density functional theory (DFT) calculations of large conjugated molecules.[62-64, 66, 69, 117] It is beyond the scope of the present manuscript deciding for the best exchange-correlation functional to characterize the electronic structure and geometry of porphyrinoids, but we believe a study of the effect of the amount of exact exchange in the aromaticity indicators is in order. Due to the relevance of the delocalization error in these measures, we will focus on the role of the exchange. To this aim, we compare the results of two popular global hybrid functionals, B3LYP and M06-2X, including 20% and 54% of exact exchange against the performance of a popular range-separated functional, CAM-B3LYP, which adds variable amounts of exchange according to the interelectronic distance considered (from 19% at short-range distances to 65% at long-range distances). In Figs. 2a and 2b, we have plotted the values of AV1245 and AV_{min} calculated with B3LYP and M06-2X against CAM-B3LYP values for all the conjugation pathways of the nine studied systems. There is an excellent agreement between M06-2X and CAM-B3LYP for both indices. However, the correlation of AV1245 values computed with

Table 3. Aromaticity indices for the annulene pathway of the nine porphyrinoid structures, calculated at the CAM-B3LYP/6-311G(d,p) level of theory. The numbers in parenthesis are the minimum value for BLA, BOA and FLU, and the maximum value for AV1245, AV_{min} and HOMA among all possible pathways.

Porphyrin	pathway	FLU	BOA	HOMA	BLA	AV1245	AV_{min}
16H	oioi	0.021	0.227 (0.000)	0.547	0.063 (0.000)	1.19 (1.58)	0.13
18H	oioi	0.010 (0.006)	0.000	0.872 (0.968)	0.000	2.16	1.28
26H	oiioii	0.019 (0.016)	0.256 (0.000)	0.716 (0.797)	0.062 (0.001)	1.58	0.61
26M	oiioii	0.028 (0.025)	0.340 (0.011)	0.542 (0.633)	0.083 (0.002)	1.02 (1.12)	0.04
28H	ooiooi	0.021 (0.017)	0.286 (0.000)	0.617 (0.759)	0.066 (0.000)	1.32 (1.46)	0.42
28M	oooioi	0.018 (0.013)	0.250 (0.000)	0.682 (0.824)	0.058 (0.000)	1.48 (1.50)	0.60
32H	ooioioi	0.023 (0.018)	0.314 (0.006)	0.594 (0.734)	0.073 (0.002)	1.18 (1.24)	0.45
32M	iooioio	0.020 (0.015)	0.263 (0.006)	0.666 (0.793)	0.062 (0.000)	1.41 (1.48)	0.55
32F	oioiooi	0.021 (0.015)	0.277 (0.000)	0.632 (0.780)	0.065 (0.001)	1.26 (1.38)	0.46

B3LYP and CAM-B3LYP presents some outliers and there is no clear correlation between the AV_{min} values predicted by both methods. In Figs. 2c and 2d, we show the same correlations but only for the annulene pathway. According to these results, the correlations are not improved when only the annulene pathway is considered. Now, we will analyze these results in greater detail.

To this aim, we have replicated the results of Table 3 with B3LYP and M06-2X in the Tables S4 and S5 of the Electronic Supplementary Information. Again, we find an excellent agreement between M06-2X and CAM-B3LYP results, suggesting that the long-range part of the exact exchange has a dominant role in the assessment of aromaticity. This finding is in line with recent results by Szczepanik *et al.*[117] Hereafter, we only discuss the differences between B3LYP and CAM-B3LYP. The analysis of specific porphyrinoid structures shows that the agreement between methods for species such as **18H** is quantitative, whereas for some other systems, such as **16H**, **26H**, **26M** and **32F**, only a qualitative agreement is observed, *i.e.*, the values are quite different between B3LYP and CAM-B3LYP but the conclusions are the same. However, there is another set of systems, including **28H**, **28M**, **32H** and **32M**, for which there is no qualitative agreement between these functionals. Indeed, B3LYP presents larger differences between aromatic and antiaromatic compounds than CAM-B3LYP and M06-2X. These results are in agreement with the recent finding that the functionals with small amounts of exact exchange tend to generate structures with bond-length equalization as opposed to the functionals with larger exchange (say, greater than 50%), which produce structures with bong-length alternation.[66] Not unexpectedly, this disagreement occurs for the most complicated systems including large porphyrinoid structures that admit Hückel, Möbius and eight-figure conformers. We have confirmed that there are non-negligible differences between the geometries predicted by B3LYP and CAM-B3LYP (or M06-2X) methods, which we speculate could be responsible for the aforementioned disagreements. These results advise some caution concerning the amount of exact exchange used in the calculation of aromatic species. Research in this line is currently underway in our laboratories.

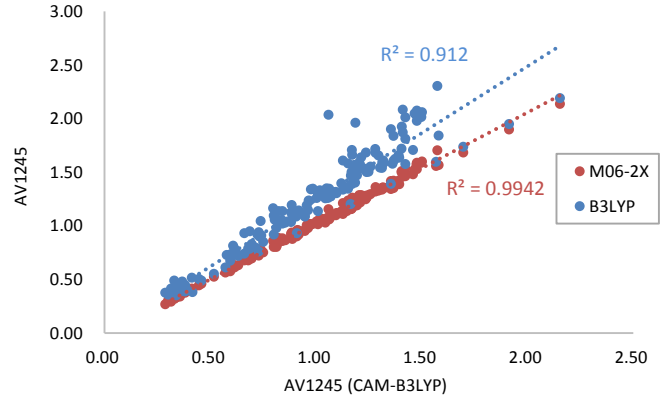

Figure 2a. Relationship between AV1245 in nine porphyrinoid compounds computed with M06-2X and B3LYP against CAM-B3LYP values for all the conjugation pathways in these structures.

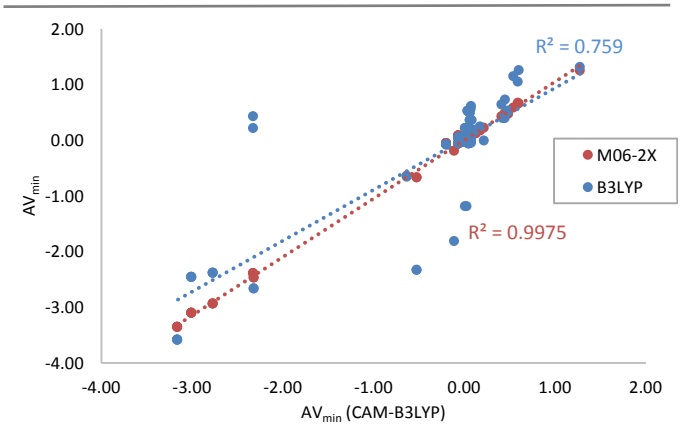

Figure 2b. Relationship between AV_{min} in nine porphyrinoid compounds computed with M06-2X and B3LYP against CAM-B3LYP values for all the conjugation pathways in these structures.

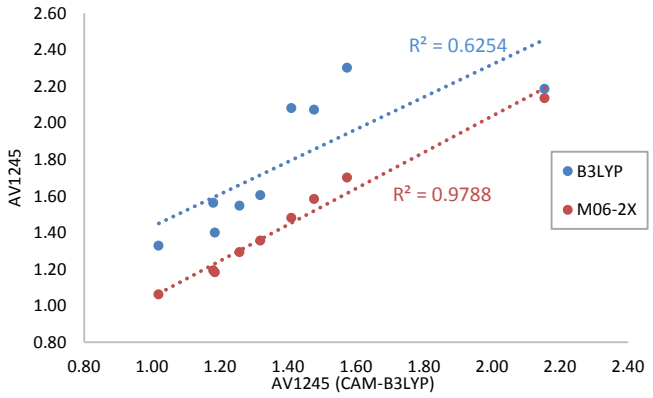

Figure 2c. Relationship between AV1245 in nine porphyrinoid compounds computed with M06-2X and B3LYP against CAM-B3LYP values for the annulene conjugation pathway in these structures.

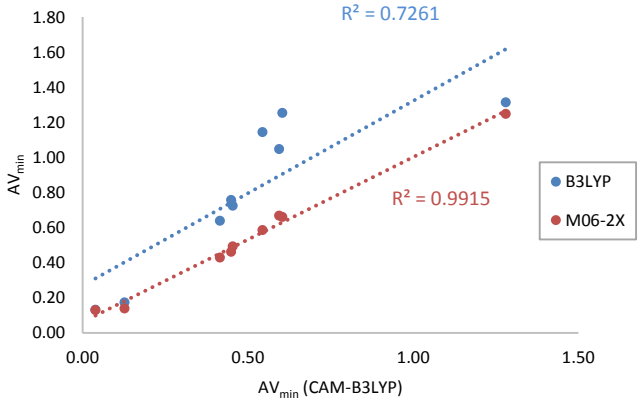

Figure 2d. Relationship between AV_{min} in nine porphyrinoid compounds computed with M06-2X and B3LYP against CAM-B3LYP values for the annulene conjugation pathway in these structures.

Conclusions

We have investigated the conjugated pathways in nine porphyrinoid compounds with varying ring size and topology using several aromaticity descriptors, including BLA, BOA, FLU and HOMA, as well as the recently introduced AV1245 and AV_{min} indices. In particular, the latter has been proposed to yield low aromaticity values for pathways with disconnected fragments that prevent a full conjugation around the macrocycle.

All the indices agree on the general features of these compounds, such as the fulfillment of Hückel's rule or which compounds should be more or less aromatic from the series. However, our results evince the difficulty in finding the most aromatic pathway in the macrocycle for large porphyrinoids. A careful examination of the data shows that some indices overestimate the aromaticity in the pathways because they are based on average values and, therefore, conceal disconnected fragments that are responsible for the loss of aromaticity. AV_{min} does not suffer from this drawback and it is actually the only index capable of recognizing the annulene pathway as the most aromatic one in the nine studied structures.

Finally, we study the effect of the exchange of DFT functionals on the description of the aromaticity of porphyrinoids. The amount of exact exchange at long range quantitatively changes the picture for most aromaticity descriptors. In line with previous findings,[66] we find that functionals with a small amount of long-range exact exchange tend to identify the macrocycles as more aromatic than functionals that include a larger percentage of exact exchange. Interestingly, regardless the method employed, AV_{min} shows the same qualitative results in all studied cases.

Conflicts of interest

There are no conflicts to declare.

Acknowledgements

Financial support was provided by the Ministerio de Economía y Competitividad (MINECO) of Spain (MINECO/FEDER projects CTQ2016-80375-P, CTQ2014-52525-P and EUIN2017-88605) and by the Eusko Jaurlaritz (Basque Government) Consolidated Group Project No. IT588-13. I.C.R. acknowledges the Basque Government for funding through a predoctoral fellowship (PRE 2016 1 0159). The authors acknowledge the computational resources and technical and human support provided by DIPC and the SGI/IZO-SGIker UPV/EHU. M. A. thanks the Fund for Scientific Research–Flanders (FWO-12F4416N) for a postdoctoral fellowship and the Free University of Brussels (VUB) for financial support.

References

1. P. v. R. Schleyer and H. Jiao, *Pure Appl. Chem.*, 1996, **68**, 209-218.
2. Z. F. Chen, C. S. Wannere, C. Corminboeuf, R. Puchta and P. v. R. Schleyer, *Chem. Rev.*, 2005, **105**, 3842-3888.
3. J. Poater, M. Duran, M. Solà and B. Silvi, *Chem. Rev.*, 2005, **105**, 3911-3947.
4. T. M. Krygowski, H. Szatylowicz, O. A. Stasyuk, J. Dominikowska and M. Palusiak, *Chem. Rev.*, 2014, **114**, 6383-6422.
5. F. Feixas, E. Matito, J. Poater and M. Solà, *WIRes Comput. Mol. Sci.*, 2013, **3**, 105-122.
6. F. Feixas, E. Matito, J. Poater and M. Solà, *Chem. Soc. Rev.*, 2015, **44**, 6434-6451.
7. M. K. Cyrański, *Chem. Rev.*, 2005, **105**, 3773-3811.
8. A. R. Katritzky, P. Barczynski, G. Musumarra, D. Pisano and M. Szafran, *J. Am. Chem. Soc.*, 1989, **111**, 7-15.
9. M. Torrent-Sucarrat, J. M. Luis and M. Solà, *Chem.-Eur. J.*, 2005, **11**, 6024-6031.
10. F. Feixas, E. Matito, J. Poater and M. Solà, *J. Comput. Chem.*, 2008, **29**, 1543-1554.
11. M. Alonso and B. Herradón, *J. Comput. Chem.*, 2010, **31**, 917-928.
12. L. Zhao, R. Grande-Aztatzi, C. Foroutan-Nejad, J. M. Ugalde and G. Frenking, *ChemistrySelect*, 2017, **2**, 863-870.

13. E. Matito, J. Poater, M. Duran and M. Solà, *J. Mol. Struct. (Theochem)*, 2005, **727**, 165-171.
14. F. Feixas, E. Matito, J. Poater and M. Solà, *J. Phys. Chem. A*, 2007, **111**, 4513-4521.
15. F. Feixas, J. O. C. Jiménez-Halla, E. Matito, J. Poater and M. Solà, *J. Chem. Theory Comput.*, 2010, **6**, 1118-1130.
16. E. Vogel, *Pure Appl. Chem.*, 1993, **65**, 143-152.
17. E. Vogel, *Angew. Chem., Int. Ed.*, 2011, **50**, 4278-4287.
18. M. K. Cyrañski, T. M. Krygowski, M. Wisiorowski, N. J. R. van Eikema Hommes and P. v. R. Schleyer, *Angew. Chem., Int. Ed.*, 1998, **37**, 177-180.
19. J. Aihara, E. Kimura and T. M. Krygowski, *Bull. Chem. Soc. Jpn.*, 2008, **81**, 826-835.
20. H. Fliegl, D. Sundholm, S. Taubert and F. Pichierri, *J. Phys. Chem. A*, 2010, **114**, 7153-7161.
21. J. Aihara, Y. Nakagami, R. Sekine and M. Makino, *J. Phys. Chem. A*, 2012, **116**, 11718-11730.
22. J. I. Wu, I. Fernández and P. v. R. Schleyer, *J. Am. Chem. Soc.*, 2013, **135**, 315-321.
23. A. S. Ivanov and A. I. Boldyrev, *Org. Biomol. Chem.*, 2014, **12**, 6145-6150.
24. R. R. Valiev, H. Fliegl and D. Sundholm, *Phys. Chem. Chem. Phys.*, 2015, **17**, 14215-14222.
25. H. Fliegl, J. Jusélius and D. Sundholm, *J. Phys. Chem. A*, 2016, **120**, 5658-5664.
26. I. Benkyi, H. Fliegl, R. R. Valiev and D. Sundholm, *Phys. Chem. Chem. Phys*, 2016, **18**, 11932-11941.
27. Y. J. Franzke, D. Sundholm and F. Weigend, *Phys. Chem. Chem. Phys*, 2017, **19**, 12794-12803.
28. M. Bröring, *Angew. Chem., Int. Ed.*, 2011, **50**, 2436-2438.
29. H. S. Rzepa, *Chem. Rev.*, 2005, **105**, 3697-3715.
30. C. S. Wannere, H. S. Rzepa, B. C. Rinderspacher, A. Paul, C. S. M. Allan, H. F. Schaefer and P. v. R. Schleyer, *J. Phys. Chem. A*, 2009, **113**, 11619-11629.
31. J. M. Lim, Z. S. Yoon, J. Y. Shin, K. S. Kim, M. C. Yoon and D. Kim, *Chem. Commun.*, 2009, 261-273.
32. M. Torrent-Sucarrat, J. M. Anglada and J. M. Luis, *J. Chem. Theory Comput.*, 2011, **7**, 3935-3943.
33. T. Woller, N. Ramos-Berdullas, M. Mandado, M. Alonso, F. de Proft and J. Contreras-Garcia, *Phys. Chem. Chem. Phys*, 2016, **18**, 11829-11838.
34. M. Torrent-Sucarrat, J. M. Anglada and J. M. Luis, *J. Chem. Phys.*, 2012, **137**, 1184306.
35. M. Torrent-Sucarrat, S. Navarro, E. Marcos, J. M. Anglada and J. M. Luis, *J. Phys. Chem. C*, 2017, **121**, 19348–19357.
36. J. Y. Shin, K. S. Kim, M. C. Yoon, J. M. Lim, Z. S. Yoon, A. Osuka and D. Kim, *Chem. Soc. Rev.*, 2010, **39**, 2751-2767.
37. S. Saito and A. Osuka, *Angew. Chem., Int. Ed.*, 2011, **50**, 4342-4373.
38. M. Stepień, N. Sprutta and L. Latos-Grażyński, *Angew. Chem., Int. Ed.*, 2011, **50**, 4288-4340.
39. T. Tanaka and A. Osuka, *Chem. Rev.*, 2017, **117**, 2584-2640.
40. B. Szyszko, M. J. Bialek, E. Pacholska-Dudziak and L. Latos-Grażyński, *Chem. Rev.*, 2017, **117**, 2839-2909.
41. Y. M. Sung, J. Oh, W. Y. Cha, W. Kim, J. M. Lim, M. C. Yoon and D. Kim, *Chem. Rev.*, 2017, **117**, 2257-2312.
42. E. Heilbronner, *Tetrahedron Lett.*, 1964, **5**, 1923-1928.
43. N. C. Baird and R. M. West, *J. Am. Chem. Soc.*, 1971, **93**, 4427-4432.
44. N. C. Baird, *J. Am. Chem. Soc.*, 1972, **94**, 4941-4948.
45. D. Ajami, O. Oeckler, A. Simon and R. Herges, *Nature*, 2003, **426**, 819-821.
46. M. Stepień, L. Latos-Grażyński, N. Sprutta, P. Chwalisz and L. Szterenberg, *Angew. Chem., Int. Ed.*, 2007, **46**, 7869-7873.
47. J. Sankar, S. Mori, S. Saito, H. Rath, M. Suzuki, Y. Inokuma, H. Shinokubo, K. S. Kim, Z. S. Yoon, J. Y. Shin, J. M. Lim, Y. Matsuzaki, O. Matsushita, A. Muranaka, N. Kobayashi, D. Kim and A. Osuka, *J. Am. Chem. Soc.*, 2008, **130**, 13568-13579.
48. Y. Tanaka, S. Saito, S. Mori, N. Aratani, H. Shinokubo, N. Shibata, Y. Higuchi, Z. S. Yoon, K. S. Kim, S. B. Noh, J. K. Park, D. Kim and A. Osuka, *Angew. Chem., Int. Ed.*, 2008, **47**, 681-684.
49. S. Tokuji, J. Y. Shin, K. S. Kim, J. M. Lim, K. Youfu, S. Saito, D. Kim and A. Osuka, *J. Am. Chem. Soc.*, 2009, **131**, 7240-7241.
50. M. Stepień, B. Szyszko and L. Latos-Grażyński, *J. Am. Chem. Soc.*, 2010, **132**, 3140-3152.
51. T. Yoneda, Y. M. Sung, J. M. Lim, D. Kim and A. Osuka, *Angew. Chem., Int. Ed.*, 2014, **53**, 13169-13173.
52. G. R. Schaller, F. Topic, K. Rissanen, Y. Okamoto, J. Shen and R. Herges, *Nature Chem.*, 2014, **6**, 609-614.
53. Y. M. Sung, M. C. Yoon, J. M. Lim, R. Rath, K. Naoda, A. Osuka and D. Kim, *Nature Chem.*, 2015, **7**, 418-422.
54. Y. Hong, J. Oh, Y. M. Sung, Y. Tanaka, A. Osuka and D. Kim, *Angew. Chem., Int. Ed.*, 2017, **56**, 2932-2936.
55. H. S. Rzepa, *Org. Lett.*, 2008, **10**, 949-952.
56. C. S. M. Allan and H. S. Rzepa, *J. Org. Chem.*, 2008, **73**, 6615-6622.
57. H. Fliegl, D. Sundholm and F. Pichierri, *Phys. Chem. Chem. Phys*, 2011, **13**, 20659-20665.
58. M. Alonso, P. Geerlings and F. de Proft, *Chem.-Eur. J.*, 2012, **18**, 10916-10928.
59. M. Alonso, P. Geerlings and F. De Proft, *J. Org. Chem.*, 2013, **78**, 4419-4431.
60. E. Marcos, J. M. Anglada and M. Torrent-Sucarrat, *J. Org. Chem.*, 2014, **79**, 5036-5046.
61. M. Alonso, B. Pinter, P. Geerlings and F. De Proft, *Chem.-Eur. J.*, 2015, **21**, 17631-17638.
62. T. Woller, J. Contreras-Garcia, P. Geerlings, F. De Proft and M. Alonso, *Phys. Chem. Chem. Phys*, 2016, **18**, 11885-11900.
63. E. Marcos, J. M. Anglada and M. Torrent-Sucarrat, *J. Phys. Chem. C.*, 2012, **116**, 24358–24366.
64. M. Alonso, P. Geerlings and F. de Proft, *Chem.-Eur. J.*, 2013, **19**, 1617-1628.
65. M. Alonso, P. Geerlings and F. De Proft, *Phys. Chem. Chem. Phys*, 2014, **16**, 14396-14407.
66. M. Torrent-Sucarrat, S. Navarro, F. P. Cossío, J. M. Anglada and J. M. Luis, *J. Comput. Chem.*, 2017, **38**, 2819–2828.
67. R. A. King, T. D. Crawford, J. F. Stanton and H. F. Schaefer, *J. Am. Chem. Soc.*, 1999, **121**, 10788-10793.
68. C. S. Wannere and P. v. R. Schleyer, *Org. Lett.*, 2004, **5**, 865-868.
69. C. S. Wannere, K. W. Sattelmeyer, H. F. Schaefer and P. v. R. Schleyer, *Angew. Chem., Int. Ed.*, 2004, **43**, 4200-4206.
70. C. Castro, W. L. Karney, M. A. Valencia, C. M. H. Vu and R. P. Pemberton, *J. Am. Chem. Soc.*, 2005, **127**, 9704-9705.
71. E. Matito, *Phys. Chem. Chem. Phys*, 2016, **18**, 11839-11846.
72. D. W. Szczepanik, M. Andrzejak, K. Dyduch, E. Zak, M. Makowski, G. Mazur and J. Mrozek, *Phys. Chem. Chem. Phys*, 2014, **16**, 20514-20523.
73. P. v. R. Schleyer, C. Maerker, A. Dransfeld, H. J. Jiao and N. Hommes, *J. Am. Chem. Soc.*, 1996, **118**, 6317-6318.
74. H. J. Dauben Jr., J. D. Wilson and J. L. Laity, *J. Am. Chem. Soc.*, 1968, **90**, 811-813.
75. F. Feixas, M. Solà, J. M. Barroso, J. M. Ugalde and E. Matito, *J. Chem. Theory Comput.*, 2014, **10**, 3055-3065.

76. R. F. W. Bader, *Atoms in Molecules: A Quantum Theory*, Clarendon, Oxford, 1990.
77. E. Matito, J. Poater, F. M. Bickelhaupt and M. Solà, *J. Phys. Chem. B*, 2006, **110**, 7189-7198.
78. E. Matito, M. Solà, P. Salvador and M. Duran, *Faraday Discuss.*, 2007, **135**, 325-345.
79. C. Foroutan-Nejad, S. Shahbazian and R. Marek, *Chem.-Eur. J.*, 2014, **20**, 10140-10152.
80. C. Foroutan-Nejad, J. Vicha, R. Marek, M. Patzschke and M. Straka, *Phys. Chem. Chem. Phys*, 2015, **17**, 24182-24192.
81. Z. Badri, C. Foroutan-Nejad, J. Kozelka and R. Marek, *Phys. Chem. Chem. Phys*, 2015, **17**, 26183-26190.
82. M. Rodríguez-Mayorga, E. Ramos-Cordoba, P. Salvador, M. Solà and E. Matito, *Mol. Phys.*, 2016, **114**, 1345-1355.
83. P. L. Bora, M. Novák, J. Novotný, C. Foroutan-Nejad and R. Marek, *Chem.-Eur. J.*, 2017, **23**, 7315-7323.
84. W. Heyndrickx, P. Salvador, P. Bultinck, M. Solà and E. Matito, *J. Comput. Chem.*, 2011, **32**, 386-395.
85. R. F. W. Bader and M. E. Stephens, *J. Am. Chem. Soc.*, 1975, **97**, 7391-7399.
86. X. Fradera, M. A. Austen and R. F. W. Bader, *J. Phys. Chem. A*, 1999, **103**, 304-314.
87. M. Rafat and L. A. Popelier, in *The quantum theory of atoms in molecules: from solid state to DNA and drug design* eds. C. F. Matta and R. J. Boyed, Wiley-VCH, Weinheim, 2007, pp. 121–140.
88. E. Francisco, D. Menéndez Crespo, A. Costales and Á. Martín Pendás, *J. Comput. Chem.*, 2017, **38**, 816-829.
89. Z. Badri and C. Foroutan-Nejad, *Phys. Chem. Chem. Phys*, 2016, **18**, 11693-11699.
90. C. Fonseca Guerra, J.-W. Handgraaf, E. J. Baerends and F. M. Bickelhaupt, *J. Comput. Chem.*, 2004, **25**, 189-210.
91. E. Matito, J. Poater, M. Solà, M. Duran and P. Salvador, *J. Phys. Chem. A*, 2005, **109**, 9904-9910.
92. E. Matito, P. Salvador, M. Duran and M. Solà, *J. Phys. Chem. A*, 2006, **110**, 5108-5113.
93. J. Kruszewski and T. M. Krygowski, *Tetrahedron Lett.*, 1972, **13**, 3839-3842.
94. T. M. Krygowski and M. K. Cyranski, *Chem. Rev.*, 2001, **101**, 1385-1419.
95. E. Matito, M. Duran and M. Solà, *J. Chem. Phys.*, 2005, **122**, 014109.
96. E. Matito, M. Duran and M. Solà, *J. Chem. Phys.*, 2006, **125**, 059901.
97. F. Feixas, M. Solà and M. Swart, *Can. J. Chem.*, 2009, **87**, 1063-1073.
98. R. Herges, *Chem. Rev.*, 2006, **106**, 4820-4842.
99. M. Giambiagi, M. S. de Giambiagi, C. D. dos Santos and A. P. de Figueiredo, *Phys. Chem. Chem. Phys.*, 2000, **2**, 3381-3392.
100. P. Bultinck, R. Ponec and S. Van Damme, *J. Phys. Org. Chem.*, 2005, **18**, 706-718.
101. X. Min, I. A. Popov, F.-X. Pan, L.-J. Li, E. Matito, Z.-M. Sun, L.-S. Wang and A. I. Boldyrev, *Angew. Chem., Int. Ed.*, 2016, **55**, 5531-5535.
102. J. Cioslowski, E. Matito and M. Solà, *J. Phys. Chem. A*, 2007, **111**, 6521-6525.
103. E. Matito, F. Feixas and M. Solà, *J. Mol. Struct. (Theochem)*, 2007, **811**, 3-11.
104. F. Feixas, E. Matito, M. Solà and J. Poater, *Phys. Chem. Chem. Phys.*, 2010, **12**, 7126-7137.
105. C. García-Fernández, E. Sierda, M. Abadía, B. Bugenhagen, M. H. Prosenc, R. Wiesendanger, M. Bazarnik, J. E. Ortega, J. Brede, E. Matito and A. Arnau, *J. Phys. Chem. C.*, 2017, DOI: 10.1021/acs.jpcc.7b08668.
106. A. D. Becke, *J. Chem. Phys.*, 1993, **98**, 5648-5652.
107. P. J. Stephens, F. J. Devlin, C. F. Chabalowski and M. J. Frisch, *J. Phys. Chem.*, 1994, **98**, 11623-11627.
108. Y. Zhao and D. G. Truhlar, *Theor. Chem. Acc.*, 2008, **120**, 215-241.
109. T. Yanai, D. P. Tew and N. C. Handy, *Chem. Phys. Lett.*, 2004, **393**, 51-57.
110. W. J. Hehre, R. Ditchfield and J. A. Pople, *J. Chem. Phys.*, 1972, **56**, 2257-2261.
111. W. J. Hehre, L. Radom, P. v. R. Schleyer and J. A. Pople, *Ab Initio Molecular Orbital Theory*, Wiley, New York, 1986.
112. In the case of the hydrogen as meso-substituent it is worth noting that the figure eight structure has almost not twist.
113. M. J. Frisch, G. W. Trucks, H. B. Schlegel, G. E. Scuseria, M. A. Robb, J. R. Cheeseman, G. Scalmani, V. Barone, B. Mennucci, G. A. Petersson, H. Nakatsuji, M. Caricato, X. Li, H. P. Hratchian, A. F. Izmaylov, J. Bloino, G. Zheng, J. L. Sonnenberg, M. Hada, M. Ehara, K. Toyota, R. Fukuda, J. Hasegawa, M. Ishida, T. Nakajima, Y. Honda, O. Kitao, H. Nakai, T. Vreven, J. A. Montgomery Jr., J. E. Peralta, F. Ogliaro, M. Bearpark, J. J. Heyd, E. Brothers, K. N. Kudin, V. N. Staroverov, R. Kobayashi, J. Normand, K. Raghavachari, A. Rendell, J. C. Burant, S. S. Iyengar, J. Tomasi, M. Cossi, N. Rega, J. M. Millam, M. Klene, J. E. Knox, J. B. Cross, V. Bakken, C. Adamo, J. Jaramillo, R. Gomperts, R. E. Stratmann, O. Yazyev, A. J. Austin, R. Cammi, C. Pomelli, J. W. Ochterski, R. L. Martin, K. Morokuma, V. G. Zakrzewski, G. A. Voth, P. Salvador, J. J. Dannenberg, S. Dapprich, A. D. Daniels, Ö. Farkas, J. B. Foresman, J. V. Ortiz, J. Cioslowski and D. J. Fox, *Gaussian 09, revision E.01, Gaussian, Inc.: Wallingford, CT*, 2009.
114. AIMAll (Version 14.11.23) aim.tkgristmill.com, Keith, T. A., TK Gristmill Software, Overland Park KS, USA , **2014**.
115. ESI-3D: Electron Sharing Indexes Program for 3D Molecular Space Partitioning, Matito, E., Institute of Computational Chemistry and Catalysis, University of Girona, Catalonia, Spain, **2014**.
116. H. Fliegl, S. Taubert, O. Lehtonen and D. Sundholm, *Phys. Chem. Chem. Phys.*, 2011, **13**, 20500-20518.
117. D. W. Szczepanik, M. Solà, M. Andrzejak, B. Pawełek, J. Dominikowska, M. Kukułka, K. Dyduch, T. M. Krygowski and H. Szatylowicz, *J. Comput. Chem.*, 2017, **38**, 1640–1654.